F. T. Arecchi
Dipartimento di Fisica
Universita di Firenze and INOA
Largo E. Fermi, 6, 50125 Firenze, Italy
E-mail: arecchi@ino.it

A. Montina
Dipartimento di Fisica
Universita di Firenze and INOA
Largo E. Fermi, 6, 50125 Firenze, Italy

Macroscopic Quantum Coherence in Bose–Einstein Condensates

Received March 30, 2003

The density of a Bose Einstein condensate (BEC) can undergo a symmetry breaking, either in real space or in momentum space. This occurs in a double well potential, obtained in real space for a BEC of lithium atoms by adding a standing wave light field to the trap potential, or in momentum space for rubidium atoms by Raman coupling two BECs in different magnetic states with two tilted light fields. Evidence of bistability results from the solution of the Gross-Pitaevskii equation. By second quantization, we show that the classical bistable situation is in fact a Schrödinger cat (SC) and we evaluate the macroscopic quantum coherence between the two SC states.

1. Introduction

The availability of Bose-Einstein condensates of trapped cold atoms with weakly repulsive or attractive mutual interactions (as e.g. respectively ^{87}Rb [1] and ^{7}Li [2]) has opened the possibility of a laboratory engineering of quantum states made of a large number of atoms [3] (around a thousand for ^{7}Li, around a milion for ^{87}Rb).

A challenging endeavour of quantum engineering is the evidence of superposition states (so called SC=Schrödinger cats) whose mutual interference is called MQC (macroscopic quantum coherence). SC have been observed for states of a trapped ion [4] and of a microwave field in a high-Q cavity [5].

Here we present the preparation of SC consisting either of a BEC of *Li* atoms split into two by a standing wave light field or of two BECs of *Rb* atoms in different internal states.

Thus far, problems related to BEC's with attractive and repulsive interactions have been treated as two different classes of problems, providing also different scenarios.

In the first case (Li), realistic calculations have been offered for macroscopic quantum tunneling (MQT) [6, 7]. Indeed, combining the kinetic and potential terms of a harmonic trap with the inter-particle attraction yields a metastable state for $N < Nc$ (Nc = critical population for an attractive BEC). Quantum tunneling from this metastable state toward the collapsed state, which would otherwise be

reached for $N > Nc$, has been shown to be feasible. Here we instead perturb the metastable state by a standing wave light field (Sec. II). This splits the condensate by an intermediate barrier, with un-equal population peaks on the two sides. As a consequence, a SC arises as the superposition of two distributions, one having the larger peak on the left of the barrier, the other on the right as the mirror image of the first one.

In this situation we predict macroscopic quantum coherence (MQC). The MQC oscillation frequency is comparable with the thermal activation energy for temperatures of a few nanokelvin, thus the effect is observable at temperatures within the reach of present technologies.

In the second case (Rb), we consider a two species BEC corresponding to two different hyperfine levels (we consider respectively $F = 1$, $m_F = -1$ and $F = 2$, $m_F = 1$). We introduce a Raman coupling between the condensates, via two optical fields L and R different in frequency and tilted with respect to each other so that there is a net momentum transfer (Sec. III). A Raman scheme for creating a superposition state (SC) between two Rb condensates at different magnetic quantum numbers has already been discussed in [8, 9]; however both papers consider co-propagating light beams. In Ref. [8], MQC is shown to require values of the scattering length between atoms of different magnetic number substantially larger than the scattering length between atoms of equal magnetic number. This requirement is too strong, since no experimental technique is today accessible to provide such a difference; furthermore if such a difference could be achieved, outstanding symmetry breaking effects would occur [10]. Ref. [9] introduces a time dependent evolution, so that SC is reached over a time of the order of 1 sec. However no clear-cut experimental test is offered to discriminate between SC and a statistical mixture of two separate states. We overcome the difficulty of Ref. [8] by introducing a suitable angular offset between the two Raman beams; this way , we show evidence of MQC between two SC, with a frequency distinguishable from thermal effects for reasonable temperatures. Furthermore we present a criterion to discriminate SC from a statistical mixture.

2. Attractive interactions

This case was already dealt with by us [11]. We refer to a condensate of ^{7}Li atoms trapped in a double well potential. A suitable model for it is given by

$$V(\vec{x}) = \frac{1}{2}m\left[\omega_{\parallel}^2 x_1^2 + \omega_{\perp}^2(x_2^2 + x_3^2)\right] + A \cdot \cos\left(2\pi\frac{x_1}{\sigma}\right). \tag{2.1}$$

The quadratic part is due to the interaction of the atoms with the magnetic field of the trap. According to laboratory implementations we choose $\omega_{\parallel} = 2\pi \cdot 130\,\mathrm{Hz}$ and $\omega_{\perp} = 2\pi \cdot 150\,\mathrm{Hz}$. The additional term is generated by two opposite laser beams in a standing wave configuration. Taking into account the interatomic interaction, the atomic system is described by a macroscopic wave function ψ which satisfies the Gross-Pitaevskii equation (GP)

$$i\hbar\frac{\partial\psi}{\partial t} = -\frac{\hbar^2}{2m}\nabla^2\psi + V\psi + g|\psi|^2\psi \equiv (H + g|\psi|^2)\psi, \tag{2.2}$$

$H = -\hbar/(2m)\nabla^2 + V$ being just the linear part of the Hamiltonian operator. Here, $m \simeq 7a.u.$ is the mass of the lithium atom, and $g = \frac{4\pi\hbar^2}{m}a$, where a is the s-wave scattering length. For a small number of atoms the GP nonlinearity can be neglected and Eq. (2.2) reduces to an ordinary Schrödinger equation. In such a case and for a sufficiently high barrier, the lowest energy level is described by a two-peak wave function symmetric with respect to inversion of the space axes, once the coordinate origin coincides with the trap center (Figure 1, dashed-dot line).

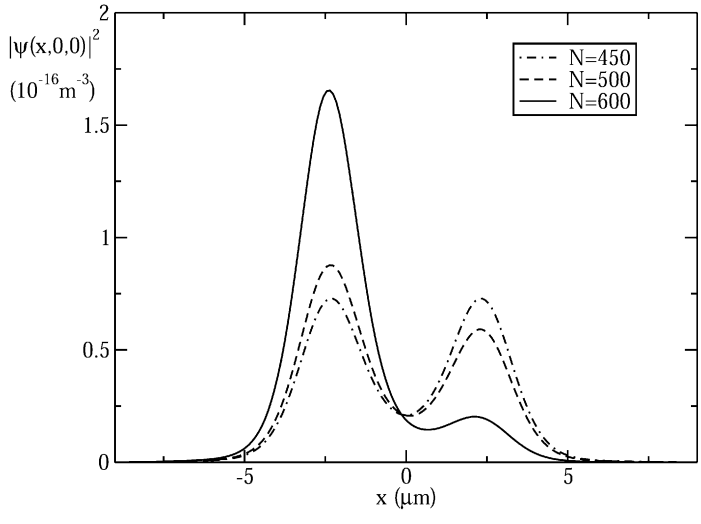

Fig. 1. Density distribution of the lithium BEC in real space for $N = 450$ (dash-dot line), $N = 500$ (dashed line) and $N = 600$ (solid line) with $A_n \equiv A/\hbar = 2650s^{-1}$ and $\sigma = 5\mu m$.

Figure 1 reports the spatial distribution of the ground state of Eq. (2.2) for different numbers of trapped atoms; the numerical method consists in solving GP on a discrete space lattice and evaluating the lowest energy state.

As we increase the number of atoms, the nonlinearity plays a relevant role. By a self consistent argument we realize that the symmetric wave function becomes unstable and we can have two new minimal energy states with distribution no longer symmetric for inversion (symmetry breaking). Indeed, assume a distribution as in Figure 1 (dashed or solid line); then the effective potential for such a distribution, due to the sum of the external potential with $g|\psi|^2$ is a double asymmetric potential well with the lower minimum corresponding to the higher population peak. For a sufficiently high nonlinear term the potential imbalance stabilizes the asymmetric distribution as in Figure 1.

We confirm the numerical calculation by the following analytic model. Let ψ_a be the equilibrium symmetrical wave function (either stable or unstable), and ψ_b be a suitable anti-symmetrical wave function such that the weighted sum of the two wave functions lowers either one of the two peaks. In the two dimensional space of these

wave functions, any other one can be expressed as

$$\psi(\vec{x}) = a\psi_a(\vec{x}) + b\psi_b(\vec{x}). \tag{2.3}$$

Without loss of generality we can choose ψ_a and ψ_b as real functions and thus consider real values for a and b. As we take $\int \psi_a^2 d^3x = \int \psi_b^2 d^3x = 1$, it follows that $a^2 + b^2 = \int \psi^2 d^3x \equiv N(a,b)$, where $N(a,b)$, the total number of atoms in the condensate, depends upon a and b. The energy is then given by

$$\mathcal{H} = a^2 H_{aa} + b^2 H_{bb} + \frac{1}{2}(a^4 I_{aa} + b^4 I_{bb}) + 3a^2 b^2 I_{ab}, \tag{2.4}$$

where

$$H_{aa} = \int \psi_a^* H \psi_a d^3x; \quad H_{bb} = \int \psi_b^* H \psi_b d^3x$$

$$I_{aa} = g \int \psi_a^4 d^3x; \quad I_{bb} = g \int \psi_b^4 d^3x$$

$$I_{ab} = g \int \psi_a^2 \psi_b^2 d^3x$$

We look for the minimal of energy with the constraint of a fixed number N of condensed atoms. These constrained minima satisfy the relations

$$\frac{\partial(\mathcal{H} - \mu N)}{\partial a} = \frac{\partial(\mathcal{H} - \mu N)}{\partial b} = 0, \tag{2.5}$$

where μ is a Lagrange multiplier. We thus solve for a and b, with the condition $N = a^2 + b^2$. The solutions $a = 0$ and $b = 0$ correspond respectively to the antisymmetric function and the symmetric one. The other solution, for both a and b nonzero, yields a^2, b^2 values as functions of μ. Using the constraint of fixed N, we eliminate μ and find

$$a^2 = \frac{H_{aa} - H_{bb} + N(3I_{ab} - I_{bb})}{6I_{ab} - I_{aa} - I_{bb}} \tag{2.6}$$

$$b^2 = \frac{H_{bb} - H_{aa} + N(3I_{ab} - I_{aa})}{6I_{ab} - I_{aa} - I_{bb}}. \tag{2.7}$$

Here the denominator is always negative. Indeed, ψ_a^2 and ψ_b^2 are almost equal at each point x. For low N, the dominant terms in the numerators have opposite sign, thus one of the two squares has to be negative, which means that there is no solution with asymmetric wave function. On the other hand, for N sufficiently large, the second term in the numerator of the two equations can compensate for the positive one, since the quantities $3I_{ab} - I_{aa}$, $3I_{ab} - I_{bb}$ are always negative.

One can easily evaluate the threshold value of N for which this symmetry breaking occurs.

In Figure 1 we report three spatial distributions of the lowest energy state. The barrier is specified by the two parameters $A/\hbar = 2650s^{-1}$ and $\sigma = 5\mu m$ (see

Eq. (2.1)). As shown in the figure, the symmetry breaking has not yet occurred for $N = 450$; instead for $N = 500$ the nonlinear term is sufficient to destabilize the symmetric state, giving rise to two asymmetric stable states. For $N = 600$ one well is almost empty.

In such a bistable situation the energy displays two minima of equal value in the infinite dimensional phase space. From a classical point of view, as the system is in its lowest energy state, the condensate is localized in either one of the two minima, where it will remain in the absence of thermal noise once we keep invariant the atom number. Since however the condensate is a mesoscopic system, quantum fluctuations play a relevant role. This can be shown by second quantization of the field, replacing the c-number macroscopic wave function by field operators.

Quantum fluctuations allow the passage from one to the other stable state without thermal activation, by pure quantum tunneling. Furthermore, due to the coherent nature of the process, we expect coherent oscillations between the two wells. Since this is not a single particle tunneling, but a tunneling of the collective variables, it is called macroscopic quantum tunneling (MQT). Since the system keeps oscillating, we will speak of macroscopic quantum coherence (MQC). We now evaluate the tunneling rate as a function of the system parameters showing the feasibility of MQC.

The most natural way of evaluating the tunneling rate consists in finding the two lowest eigenvalues of the Hamiltonian and taking their difference. Indeed, the sum and difference of the corresponding states are respectively the alive and dead state of SC, and the transition time is half a period corresponding to the frequency difference.

The problem is simplified by reducing it to two degrees of freedom by the expansion Eq.(2.3).

We select the basis functions ψ_a and ψ_b as follows. Calling $\psi_0(\vec{x})$ the minimal energy wavefunction of the GP problem (see e.g. Figure 1), we take for ψ_a and ψ_b respectively the symmetric and antisymmetric sums $\psi_0(\vec{x}) \pm \psi_0(-\vec{x})$. Expansion (2.3) with these ψ_a and ψ_b includes the original functions $\psi_0(\vec{x})$ and $\psi_0(-\vec{x})$ for suitable values of a and b. Furthermore, it simplifies the form of the Hamiltonian as we see right now.

In second quantization, a and b in Eq. (2.3) have to be taken as operators $\hat{a}$ and $\hat{b}$, obeying Bose commutation rules with their conjugate $\hat{a}^\dagger$, $\hat{b}^\dagger$. Exploiting the operator version of Eq. (2.3) and its adjoint, the Hamiltonian becomes

$$\mathcal{H} = \hat{a}^\dagger \hat{a} H_{aa} + \hat{b}^\dagger \hat{b} H_{bb} + \frac{1}{2}(\hat{a}^{\dagger 2}\hat{a}^2 I_{aa} + \hat{b}^{\dagger 2}\hat{b}^2 I_{bb}) + \left(\frac{1}{2}\hat{a}^{\dagger 2}\hat{b}^2 + \frac{1}{2}\hat{b}^{\dagger 2}\hat{a}^2 + 2\hat{a}^\dagger \hat{b}^\dagger \hat{a}\hat{b}\right) I_{ab}, \tag{2.8}$$

where the coefficients H_{aa}, H_{bb}, I_{aa}, I_{bb} and I_{ab} are the same as in Eq. (2.4).

We consider the basis of eigenvectors of the number operators

$$|0, N\rangle, |1, N-1\rangle, \ldots |N, 0\rangle, \tag{2.9}$$

where $\hat{a}^\dagger \hat{a}|k, m\rangle = k|k, m\rangle$ and $\hat{b}^\dagger \hat{b}|k, m\rangle = m|k, m\rangle$. Let us call

$$H_{l,k} = \langle l, N-k|\mathcal{H}|k, N-k\rangle \tag{2.10}$$

the generic matrix element of the Hamiltonian on the above basis. We evaluate the eigenvalues of this matrix. In Figure 2 we plot the first and second excited energy levels versus N for different parameters A and σ of the applied field.

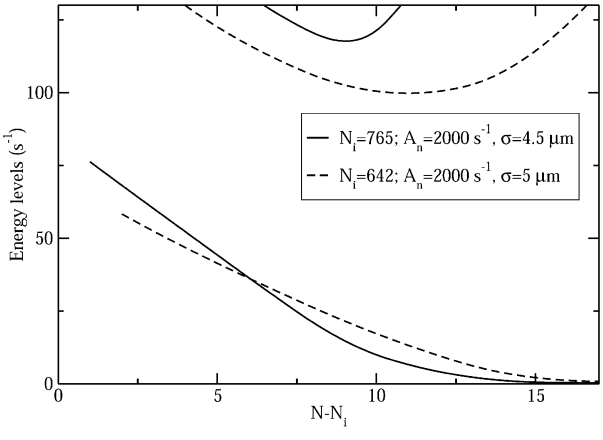

Fig. 2. First and second energy levels of the lithium BEC versus the excess of atoms above the breakup value N_i.

In the number representation there is no explicit evidence of a Schrödinger cat (SC) as a two-peak distribution. We look for a suitable observable, whose probability distribution provides such an evidence. We take the first component of the barycenter coordinate $x_c = 1/N \int x_1 |\psi|^2 d^3x$ as the appropriate variable since the corresponding classical states (minima of the Hamiltonian (2.4)) have separated barycenters. It is associated with the operator

$$\hat{x}_c = \frac{1}{N} \int x_1 \psi_a(\vec{x}) \psi_b(\vec{x}) d^3x (\hat{a}^\dagger \hat{b} + \hat{a}\hat{b}^\dagger). \tag{2.11}$$

Besides a c-number factor, the observable is thus $\hat{M} = \hat{a}^\dagger \hat{b} + \hat{a}\hat{b}^\dagger$. The associated probability density is $P(m) = |\langle m|\phi_0\rangle|^2$, where $|\phi_0\rangle$ is the ground state of Hamiltonian (2.8) and $|m\rangle$ is the eigenstate of $\hat{M}$ with eigenvalue m. Notice that once the number of atoms is fixed the eigenvectors are not degenerate.

Since we know the components of $|\phi_0\rangle$ on the number basis we must express $|m\rangle$ with respect to that basis, that is,

$$|m\rangle = \sum_k c_k^m |k, N-k\rangle. \tag{2.12}$$

Applying the operator $\hat{M}$ to the above ket we have

$$m|m\rangle = \sum_k c_k^m (\hat{a}^\dagger \hat{b} + \hat{a}\hat{b}^\dagger)|k, N-k\rangle. \tag{2.13}$$

Projecting on $\langle l, N-l|$ the above ket it follows that

$$\sum_k M_{l,k} c_k^m = m c_l^m, \tag{2.14}$$

where

$$M_{l,k} = \langle l, N-l|\hat{M}|k, N-k\rangle. \tag{2.15}$$

Since $M_{l,k}$ are known, solving the eigenvector equation (2.14) we can evaluate the coefficients c_k^m and hence $P(m)$.

The two-peak distribution $P(m)$ is plotted in Figure 3 for different N values and for $A/\hbar = 2000 s^{-1}$, $\sigma = 4.5 \mu m$.

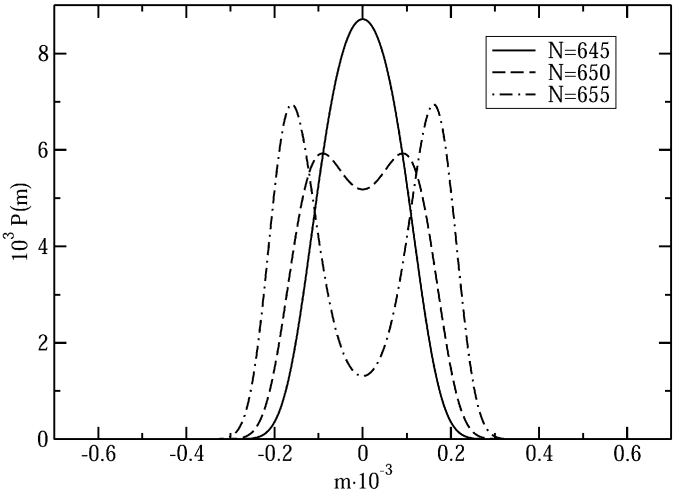

Fig. 3. Probability distribution of the "barycenter" indicator for the lithium BEC in the SC situation, for three different N values and for a standing wave with $A_n = 2000 s^{-1}$ and $\sigma = 5 \mu m$.

Experimentally, evidence of SC against a trivial statistical mixture is obtainable by setting the system at the above parameter values and observing the coherent oscillation between the two energy minima by a measurement not destroying the coherence (e.g. a phase contrast technique). The preparation process provides a superposition of the ground state $\phi_0(m)$ and the first excited state $\phi_1(m)$. The symmetry of Hamiltonian (2.8) with respect to an exchange of $\hat{a}$ and $\hat{b}$ shows that $\phi_0(m)$ is symmetric and $\phi_1(m)$ antisymmetric. Taking ϕ_0 and ϕ_1 as real functions the superposition at $t = 0$ is $\phi_0(m) + \phi_1(m)$. After half a period corresponding to the frequency separation ω_f between ground and first excited state, the superposition will be $\phi_0(m) - i\phi_1(m)$ and the corresponding probability is the two peak aspect

$$Q(m, t = \pi/\omega_f) = \phi_0(m)^2 + \phi_1(m)^2. \tag{2.16}$$

Notice that the simple sum rule implies the evidence of two distinct peaks in $Q(m)$ even when the energy of the ground state is still below the barrier. Indeed in such a case, $P(m)$ is flat at the origin; however $\phi_1(m)$ is zero at $m = 0$ and hence its square has two separate peaks which show up in (2.16).

In conclusion, we have demonstrated the feasibility of MQC between the two minima of a BEC of ^7Li atoms in the presence of an applied standing wave laser. The oscillation frequency between the two states of the SC is $\omega_f \sim 50s^{-1}$ (see Figure 2 for $N - N_i \sim 5$). In order to prepare states with such a separation and yet neglect thermal activation, the system should be cooled at a temperature of around $1nK$. To cool at $1nK$ is within the reach of present technologies, even though such a low temperature has not yet been reported.

3. Repulsive interactions

In the case of ^{87}Rb, we apply two Raman fields L and R and adjust the frequency difference in order to quasi-resonantly couple two different hyperfine levels.

For low condensate densities, the presence of such a pair of fields gives rise to a two branch atomic dispersion curve, the lower branch having two minima, corresponding to two distinct condensate states between which it is possible to have single particle quantum tunneling. The nonlinear interaction term tends to contrast the quantum tunneling, clustering the atoms in only one of the two potential wells. Adjusting the frequency offset with respect to the matching conditions leads to a critical value above which only one stable solution exists for the condensate. As the frequency variation is changed in the other sense, an hysteresis cycle appears, showing evidence of bistability.

This suggests the possibility of a MQC. In the limit where the two quantum states become no longer superposed, the MQC reduces to a classical bistability.

We call ψ_0 and ψ_1 the fields representative of the condensate states corresponding to the $F = 1$, $m_F = -1$ and $F = 2$, $m_F = 1$ levels, respectively. Furthermore we call ψ_2 the upper state of the D_1 transition.

The starting equations are

$$i\hbar\frac{\partial\psi_0}{\partial t} = H_0[\psi_0,\psi_1]\psi_0 + \hbar E_L(t)e^{-i(\vec{k}_L\cdot\vec{x}-\omega_L t)}\psi_2 \tag{3.1}$$

$$i\hbar\frac{\partial\psi_1}{\partial t} = H_1[\psi_0,\psi_1]\psi_1 + \hbar E_R(t)e^{-i(\vec{k}_R\cdot\vec{x}-\omega_R t)}\psi_2 + \hbar\omega_1\psi_1 \tag{3.2}$$

$$i\hbar\frac{\partial\psi_2}{\partial t} = \hbar\omega_2\psi_2 + \hbar E_L^*(t)e^{i(\vec{k}_L\cdot\vec{x}-\omega_L t)}\psi_0 + \hbar E_R^*(t)e^{i(\vec{k}_R\cdot\vec{x}-\omega_R t)}\psi_1, \tag{3.3}$$

where

$$H_0[\psi_0,\psi_1] = H_L + g_{00}|\psi_0|^2 + g_{01}|\psi_1|^2 \tag{3.4}$$

$$H_1[\psi_0,\psi_1] = H_L + g_{11}|\psi_1|^2 + g_{10}|\psi_0|^2. \tag{3.5}$$

We have called

$$H_L = -\frac{\hbar^2}{2m}\nabla^2 + V \tag{3.6}$$

the linear part of the Hamiltonian, where V is the trapping potential, which is the same for the two states since it depends only on m_F. The field amplitudes $E_{L,R}$ are rescaled in order to be expressed in frequency units. They are thus the Rabi frequencies of the one-photon transition.

$\hbar\omega_2$ is the energy of the upper state of the one photon transition; $\hbar\omega_1$ is the energy of the $F = 2$, $m_F = 1$ level; the $F = 1$, $m_F = -1$ level energy is set to zero. In Eqs. (3.4,3.5) $g_{ij} = 4\pi\hbar^2 a_{ij}/m$ where a_{ij} is the s-wave scattering length which depends upon the selected state. Precisely $a_{00} = 5.68nm$ for two atoms in the $F = 1$, $m_F = -1$ state, $a_{11} = 5.36nm$ for two atoms in the $F = 2$, $m_F = 1$ state and $a_{01} = a_{10} = 5.52nm$ for one atom in the first and the other in the second state [10].

In the adiabatic approximation, ψ_2 can be expressed in terms of ψ_1 and ψ_0 as follows

$$\psi_2 = -\frac{1}{\Delta}[E_L^* e^{i(\vec{k}_L\cdot\vec{x}-\omega_L t)}\psi_0 + E_R^* e^{i(\vec{k}_R\cdot\vec{x}-\omega_R t)}\psi_1], \tag{3.7}$$

where $\Delta = \omega_2 - \omega_L$. Thus we have two closed equations for ψ_0 and ψ_1. Introduce the transformation

$$\tilde{\psi}_0 = e^{i\int\frac{|E_L|^2}{\Delta}dt} e^{i(\frac{\vec{k}_d}{2}\cdot\vec{x}-\frac{\omega_d}{2}t+\frac{\hbar\vec{k}_d^2}{8m}t)}\psi_0 \tag{3.8}$$

$$\tilde{\psi}_1 = e^{i\int\frac{|E_R|^2}{\Delta}dt} e^{-i(\frac{\vec{k}_d}{2}\cdot\vec{x}-\frac{\omega_d}{2}t-\frac{\hbar\vec{k}_d^2}{8m}t)}\psi_1, \tag{3.9}$$

where $\vec{k}_d = \vec{k}_L - \vec{k}_R$ and $\omega_d = \omega_L - \omega_R$. Assuming $|E_R| = |E_L|$, the equations of motions become

$$i\hbar\frac{\partial\tilde{\psi}_0}{\partial t} = H_0[\tilde{\psi}_0,\tilde{\psi}_1]\tilde{\psi}_0 - \hbar\Omega\tilde{\psi}_1 - \frac{\hbar\delta}{2}\tilde{\psi}_0 + \frac{i\hbar^2\vec{k}_d\cdot\vec{\nabla}}{2m}\tilde{\psi}_0 \tag{3.10}$$

$$i\hbar\frac{\partial\tilde{\psi}_1}{\partial t} = H_1[\tilde{\psi}_0,\tilde{\psi}_1]\tilde{\psi}_1 - \hbar\Omega^*\tilde{\psi}_0 + \frac{\hbar\delta}{2}\tilde{\psi}_1 - \frac{i\hbar^2\vec{k}_d\cdot\vec{\nabla}}{2m}\tilde{\psi}_1. \tag{3.11}$$

Here, $\Omega \equiv \frac{E_L E_R^*}{\Delta}$ is the two photon Rabi frequency taken for simplicity as time independent and real and the frequency δ is given by

$$\delta = \omega_1 - \omega_d. \tag{3.12}$$

If the number of atoms is sufficiently small, we can neglect the nonlinear terms. Furthermore, let us initially consider a spatially homogeneous condensate (no trap potential). As a consequence, Eqs. (3.10) and (3.11) reduce to two linear equations with constant coefficients, and the eigenvalue problem in the reciprocal space is ruled by two linear algebraic equations in the transformed fields $\phi_0(\vec{k})$ and $\phi_1(\vec{k})$. The impulses corresponding to the two levels $F = 1$ and $F = 2$ are respectively $\hbar(\vec{k} - \vec{k}_d/2)$ and $\hbar(\vec{k} + \vec{k}_d/2)$. Solving the eigenvalue problem we find two dispersion curves

$$\hbar\omega(\vec{k}) = \frac{\hbar^2\vec{k}^2}{2m} \pm \sqrt{\left(\frac{\hbar^2\vec{k}_d\vec{k}}{2m} + \frac{\hbar\delta}{2}\right)^2 + \hbar^2|\Omega|^2}. \tag{3.13}$$

In Figure 4 we have plotted the two curves for $\Omega = 60Hz$ and $|\vec{k}_d| = 2\pi\cdot 1.2\cdot 10^5 m^{-1}$.

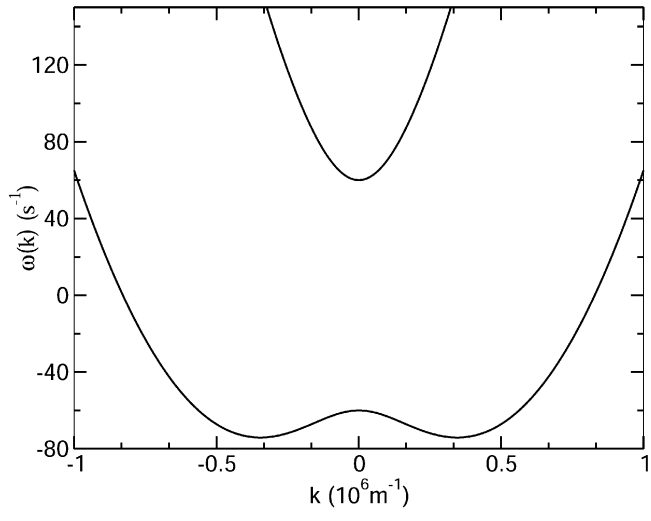

Fig. 4. Dispersion curves for a double rubidium BEC with magnetic states $F = 1$, $m_F = -1$ and $F = 2$, $m_F = 1$ in the presence of Raman fields with $|\vec{k}_d| = 2\pi \cdot 1.2 \cdot 10^5 m^{-1}$ and $\Omega = 60Hz$.

As shown in the figure, the electromagnetic coupling modifies the parabolic dispersion curves associated with the two hyperfine levels, lifting the degeneracy at their intersection point. The energy gap for $\delta = 0$ is $2\hbar|\Omega|$. By varying δ one can rise or lower the energy separation between the two minima, which for $\delta = 0$ are aligned.

Introducing the harmonic trap potential, the fundamental state has no longer a definite impulse. Furthermore, the two wells of the dispersion curve are equally populated by quantum tunneling.

An interesting phenomenon occurs when the interatomic interaction is no longer negligible. We report in Figure 5 the distributions $|\phi_0|^2$ and $|\phi_1|^2$ for $\delta = 0$ and for three different values of N. ϕ_0 and ϕ_1 are the Fourier transforms of the ground state solution $(\tilde{\psi}_0, \tilde{\psi}_1)$ of Eqs. (3.10,3.11), evaluated numerically on a lattice. As it results, this interaction clusters the majority of atoms within a single well, thus contrasting the quantum tunneling across the barrier.

Due to the geometry of the problem, and taking into account that the three scattering lengths a_{00}, a_{11} and a_{01} (respectively for two atoms in state F_1, for two atoms in state F_2, and for one in F_1 and one in F_2) are practically equal, there is another ground state which is obtained from that of Figure 5 by inverting the horizontal axis and interchanging ϕ_0 and ϕ_1. Thus we have two stable stationary states with almost equal energy (exactly at the same energy if we take all scattering lengths equal). This is a bistability case.

In summary, we have shown evidence of the coexistence of two states.

The numerical evidence of Figure 5 is also supported by a synthetic variational argument, as the same adopted for Li in the previous section.

To provide evidence of MQC we quantize the two mode system as done for Li in Sec. II.

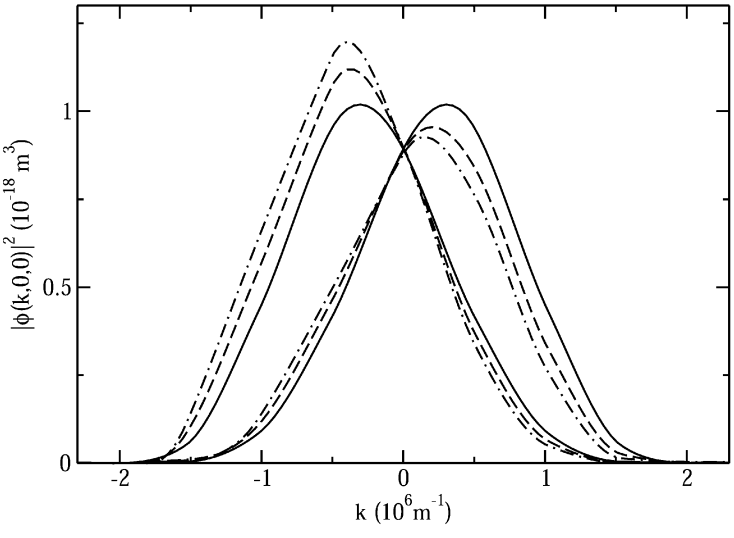

Fig. 5. Density distributions of the rubidium BEC for Raman fields with $k_d = 4.5 \cdot 10^5 m^{-1}$ and two photon Rabi frequency $\Omega = 1100 s^{-1}$ and three different condensate numbers: $N =$ $= 1390$ (solid), 1420 (dashed), 1460 (dot-dashed).

First of all, we write the classical Hamiltonian corresponding to the equations of motions (3.10,3.11), taking for simplicity $g_{00} = g_{11} = g_{01} \equiv g$ and $\delta = 0$

$$\mathcal{H} = \int \Big[\psi_0^* H_L \psi_0 + \psi_1^* H_L \psi_1 + + g\left(\frac{1}{2}|\psi_0|^4 + \frac{1}{2}|\psi_1|^4 + |\psi_0|^2|\psi_1|^2\right) + \\ + \frac{i\hbar^2 \vec{k}_d}{2m}(\psi_0^* \vec{\nabla}\psi_0 - \psi_1^* \vec{\nabla}\psi_1) - \hbar\Omega(\psi_1^*\psi_0 + \psi_0^*\psi_1)\Big] d^3x \quad (3.14)$$

(for simplicity, from now on we omit the tilde on the ψ's, even though we are always in the gauge (3.8), (3.9)).

We then generalize to a spinorial space the choice of the basis wave-functions ψ_a and ψ_b.

Let us introduce the spinorial ground state

$$\vec{\psi}_{g,1}(\vec{x}) \equiv \begin{pmatrix} \psi_{0g}(\vec{x}) \\ \psi_{1g}(\vec{x}) \end{pmatrix}, \quad (3.15)$$

where ψ_{0g} and ψ_{1g} are the two ground state wave-functions associated with the two magnetic states.

The second ground state of the Hamiltonian (3.14) is

$$\vec{\psi}_{g,2}(\vec{x}) \equiv \begin{pmatrix} \psi_{1g}(-\vec{x}) \\ \psi_{0g}(-\vec{x}) \end{pmatrix}. \quad (3.16)$$

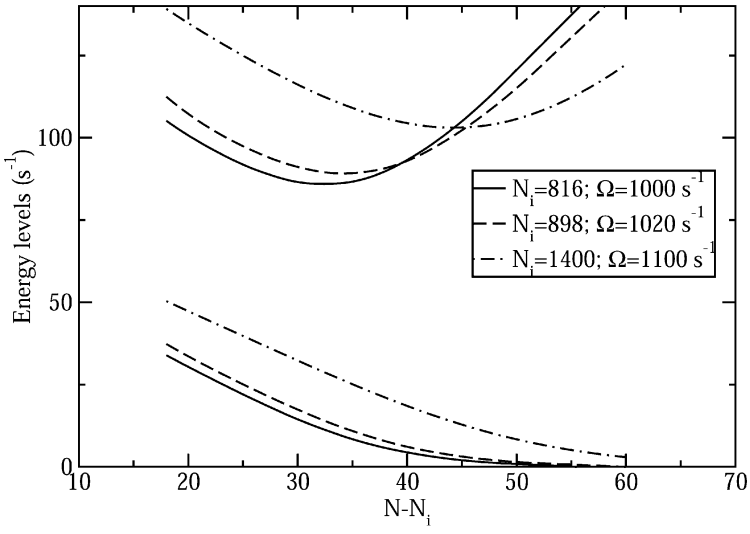

Fig. 6. First and second energy levels of the rubidium BEC versus the excess of atoms above the breakup value N_i.

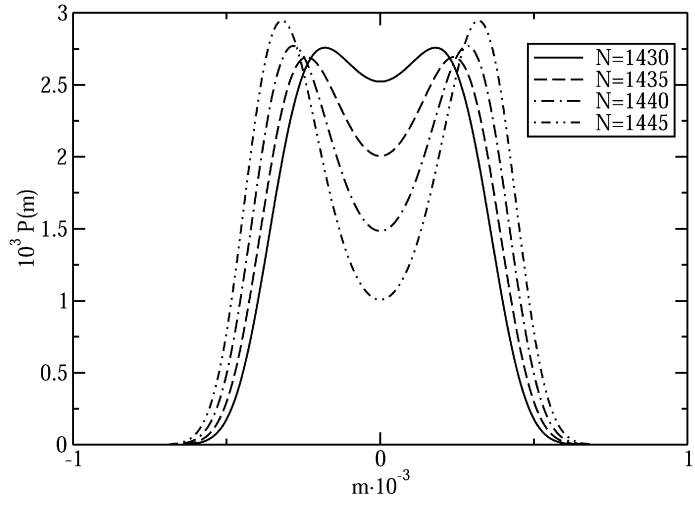

Fig. 7. Probability distribution of the "barycenter" indicator for the rubidium BEC in the SC situation, for four different N values and for $k_d = 4.5 \cdot 10^5 m^{-1}$.

With these spinorial ground states, the spinorial version of ψ_a and ψ_b of section II are respectively

$$\vec{\psi}_a = \vec{\psi}_{g,1} + \vec{\psi}_{g,2} \tag{3.17}$$

$$\vec{\psi}_b = \vec{\psi}_{g,1} - \vec{\psi}_{g,2}. \tag{3.18}$$

Thus, Eq. (2.3) generalizes to

$$\vec{\psi}(\vec{x}) = a\vec{\psi}_a(\vec{x}) + b\vec{\psi}_b(\vec{x}). \tag{3.19}$$

In second quantization, we take a and b as operators and the associated Hamiltonian is again Eq. (2.8), with the coefficients evaluated on the new basis.

Having established the new rules, we now repeat the same steps done in Sec. II. Precisely, we evaluate the difference between the lowest eigenvalues which provides the tunneling rate and plot it in Figure 6. Furthermore, we plot in Figure 7 $P(m)$ versus m, the definitions being the same as in the previous section.

4. Conclusion

We have shown evidence of SC in Bose Condensates of atoms, both in the attractive and repulsive case. In the attractive case (Li) we have split the BEC by the introduction of a standing wave of light. In the repulsive case (Rb) we start from two BECs in different magnetic states and introduce a Raman coupling via two tilted light fields, which provide a momentum transfer between the two condensate.

In both cases, we introduce a suitable indicator which yields evidence of MQC against the trivial case of two states in a statistical mixture. The tunneling rates between alive and dead SC are within the reach of present laboratory technologies.

References

[1] M. H. Anderson, J. R. Ensher, M. R. Matthews, C. E. Wieman, and E. A. Cornell, Science, **269**, 198 (1995).
[2] C. C. Bradley, C. A. Sackett, and R. G. Hulet, Phys. Rev. Lett., **78**, 985 (1997).
[3] R. Walsworth and L. You, Phys. Rev. A, **56**, 555 (1997).
[4] C. Monroe et al., Science, **272**, 1131 (1996).
[5] M. Brune et al., Phys. Rev. Lett., **77**, 4887 (1996).
[6] M. Ueda and A. J. Leggett, Phys. Rev. Lett., **80**, 1576 (1998).
[7] L. Salasnich, Phys. Rev. A, **61**, 015601 (1999).
[8] J. I. Cirac et al., Phys. Rev. A, **57**, 1208 (1998).
[9] D. Gordon and C. M. Savage, Phys. Rev. A, **59**, 4623 (1999).
[10] D. Gordon and C. M. Savage, Phys. Rev. A, **58**, 1440 (1998).
[11] A. Montina and F. T. Arecchi, Phys. Rev. A, accepted for publication.